arXiv:cond-mat/0303037v1 [cond-mat.stat-mech] 3 Mar 2003

# Kinetics of Fragmenting Freely Evolving Granular Gases

Ignacio Pagonabarraga,
Departament de Física Fonamental, Universitat de Barcelona
Carrer Martí i Franqués, 1, 08028-Barcelona, Spain
and
Emmanuel Trizac
Laboratoire de Physique Théorique (UMR 8627 du CNRS), Bâtiment 210,
Université de Paris-Sud, 91405 Orsay Cedex, France

**Summary.** We investigate the effect of fragmentation on the homogeneous free cooling of inelastic hard spheres, using Boltzmann kinetic theory and Direct Monte Carlo simulations. We analyze in detail a model where dissipative collisions may subsequently lead to a break-up of the grains. With a given probability, two offsprings are then created from one of the two colliding partners, with conservation of mass, momentum and kinetic energy. We observe a scaling regime characterized by a single collisional average, that quantifies the deviations from Gaussian behaviour for the joint size and velocity distribution function. We also discuss the possibility of a catastrophe whereby the number of particles diverges in a finite time. This phenomenon appears correlated to a "shattering" transition marked by a delta singularity at vanishingly small grains for the rescaled size distribution.

## 1 Introduction

The phenomenon of fragmentation is central to many natural and technological processes, from geology to the pharmaceutical industry (where e.g. the properties of an active principle depend on the size distribution of its constituents). In the realm of granular gases where the fluidization is achieved by a violent excitation or shaking, the fragmentation mechanism is also relevant although experimental studies of these systems usually avoid such a complication.

A theoretical description of fragmentation is nevertheless a difficult task and traditional approaches rely on rate (Smoluchowski-like) equations [1], that describe the time evolution of the size distribution after having integrated out the other degrees of freedom, such as the velocities of the particles. However, when the motion between the collision events is free, the dynamics of a reacting system in general (where, because of collisions, particles may break up, aggregate, annihilate ...) is determined by details of the collision (collisional correlations [2]) which often invalidate the rate equation approach, at least in its usual version. In particular, for dynamics that do not conserve the number of particles, the time evolution of the density crucially depends on the ratio of the kinetic energy dissipated in a "typical" collision, to the mean kinetic energy of the particles [2,3]. It therefore appears that a more microscopic description than the coarse grained rate equation route is

necessary, at the expense of a non negligible complication. When particles disappear upon colliding, it is however possible to prove that the Boltzmann equation becomes exact at late times (in space dimensions $D > 1$ [3]). Although it does not seem possible to show that the validity of Boltzmann's picture (which is less restrictive than the Smoluchowski approach) pertains to a modification of the reaction rule, such an approach captures important collisional correlations missed by the naive rate equation framework. In the following analysis, we will therefore use Boltzmann's kinetic theory (relying on the molecular chaos assumption that the 2 body distribution function of colliding pairs may be factorized in terms of the single particle distribution [4]), to investigate the dynamics of a fragmenting granular gas.

## 2 Model

We consider a gas of grains that evolve freely in time, from an initial equilibrium distribution, i.e. we assume that up to the initial time, the system is elastic, and hence, that its velocity distribution is Maxwellian.

In the fluidized regime we shall be interested in, grains interact as hard bodies; collisions are always binary, and instantaneous. In a $D$-dimensional system, at each collision a fraction $(1-\alpha^2)/(2D)$ of the relative kinetic energy is lost, where $\alpha$, the inelasticity (or restitution) coefficient, measures the departure from elastic behaviour. After each collision, the stored kinetic energy in internal grain excitations may lead to a break-up of the grains. Such a fragmentation event is stochastic in nature. Previous studies suggest than in a number of materials, the probability that a grain breaks is related to the number of surface defects (or micro-cracks). The more kinetic energy is dissipated, the larger the chance that one of such defects enlarges, leading to the break-up of the grain. Hence, the fracture probability is related both to the energy lost and to the defect distribution (and the related surface stress distribution). There exist different models in the literature that account for such effects. A reasonable fragmentation probability model assumes that the stored energy and the defect distribution are uncorrelated, and that defects are uniformly distributed over a particle's surface; the breaking probability is thus proportional to the particle's surface [6]. Once a grain breaks, we should also specify the number of out-coming particles, and how their sizes and velocities are related to the physical properties of the fragmenting grain. Here the situation is more controversial, and it is highly dependent on whether the breaking process is induced by an energy input from a source which drives the system or whether it is due to the internal dynamics of the system; despite this, the Roslin-Rammler law (and a few variants) is considered to be a reasonable description for the off-spring distribution[1,6].

Rather than attempting a detailed description of the fragmentation mechanism, in this paper we will assume the simplest break-up process. The idea is to minimize the amount of input at the collision level and to analyze which is the behavior of the system under the simplest possible mechanical rules. We hope to be able to carry out a detailed analysis that will be helpful before investigating more refined approaches.

In our model, after the collision has taken place, with a probability $p$ we break one of the two colliding grains. The grain fragments in 2 off-springs which keep the (spherical) shape of the parent grain. The fragmentation process conserves mass, momentum and kinetic energy. The mass is distributed randomly between the two

out-coming grains with a uniform probability density. In this case, the conservation of momentum and kinetic energy imply that both off-springs have the same velocity, equal to that of the fragmenting grain. If we would assume that the two colliding grains may break up due to the collision, there would exist more freedom in the velocity redistribution of the off-springs, even assuming coplanarity of the out-coming grains' trajectories. We will consider that the mass density of the grains is conserved, so that the relation between mass $m$ and radius $\sigma$ is taken as $m = \sigma^D$.

We will further concentrate on the homogeneous freely evolving state of the fluid under consideration. Such a situation has received much attention in the absence of fragmentation, and the theoretical predictions have been contrasted against molecular dynamics simulations. The homogeneous state is known to be unstable against low wave length fluctuations of the vorticity, and at late times, hydrodynamic flows set up[5]. As a first step, we will concentrate in the regime prior to the appearance of the hydrodynamic instability. In fact, having a hydrodynamics origin, we might also expect an analogous instability in the present model.

In this homogeneous state, the Boltzmann equation, which determines, at a mean-field level, the time evolution of the system through the one-particle distribution function $f(\boldsymbol{v}, \sigma, t)$, in a $D$-dimensional space has the form

$$\begin{aligned}\frac{\partial f(\boldsymbol{v},\sigma,t)}{\partial t} = \frac{1}{2}\int dug(u)\int d\boldsymbol{v}_1 d\boldsymbol{v}_2 d\sigma_1 d\sigma_2 d\widehat{\varepsilon}\ \theta(\boldsymbol{v}_{12}\cdot\widehat{\varepsilon})\,|\boldsymbol{v}_{12}\cdot\widehat{\varepsilon}|\,\sigma_{12}^{D-1}\,\{ \\ f(\boldsymbol{v}_1,\sigma_1,t)f(\boldsymbol{v}_2,\sigma_2,t)\,[-\delta(\boldsymbol{v}-\boldsymbol{v}_1)\delta(\sigma-\sigma_1)-\delta(\boldsymbol{v}-\boldsymbol{v}_2)\delta(\sigma-\sigma_2) \\ +\quad (1-p)\delta(\boldsymbol{v}-\boldsymbol{v}_1^*)\delta(\sigma-\sigma_1)+(1-p)\delta(\boldsymbol{v}-\boldsymbol{v}_2^*)\delta(\sigma-\sigma_2) \\ +\quad p\delta(\boldsymbol{v}-\boldsymbol{v}_1^*)\left[\delta(\sigma-\sigma_1\cdot u^{1/D})+\delta(\sigma-\sigma_1\cdot(1-u)^{1/D})\right] \\ +\quad p\delta(\boldsymbol{v}-\boldsymbol{v}_2^*)\left[\delta(\sigma-\sigma_2\cdot u^{1/D})+\delta(\sigma-\sigma_2\cdot(1-u)^{1/D})\right]\Big]\Big\} \qquad (1)\end{aligned}$$

In the previous expression, $\boldsymbol{v}$ stands for the velocity, $\sigma$ for the particles' radius, while $\widehat{\varepsilon}$ is a unit vector joining the centers of the colliding grains. The Heaviside function, $\theta$, ensures the appropriate kinematic constraint, that only approaching grains will collide, while the term $|\boldsymbol{v}_{12}\cdot\widehat{\varepsilon}|\,\sigma_{12}^{D-1}$ is the collision cross-section; the subscript 12 refers to the difference between the values of the colliding pair, e.g. $\boldsymbol{v}_{12} = \boldsymbol{v}_1 - \boldsymbol{v}_2$. Moreover, $g(u)$ is the probability density that one of the off-springs, in case of fragmentation, has a mass $u$ times the parent's mass. Due to mass conservation, $g(u) = g(1-u)$. In the model analyzed below, we consider the simplest case where this distribution is uniform [$g(u) = 1$ and $0 \le u \le 1$].

For clarity's sake, we have expressed the general evolution equation in terms of the elementary processes affecting the two colliding grains. Obviously, a simplified expression can be derived using the symmetric role that the two grains play during the collision.

The first two terms in the r.h.s. of (1) account for the disappearance of particles of a given velocity due to the collision process itself. For the same reason, new particles of a given species and velocity are produced at the collision. These terms involve the precollision velocities, $\boldsymbol{v}^*$, because we require that the out-coming velocity of the collision corresponds to the velocity $\boldsymbol{v}$. It is through these, precollisonal velocities, that the inelastic character of the collision enters. Indeed, the precollision velocities, in terms of the post-collisional ones (which are the relevant velocities in the previous kinetic equation in order to describe the kinetic processes), are given

by

$$\boldsymbol{v}_{1,2}^{*} = \boldsymbol{v}_{1,2} \mp \frac{m_2}{m_1+m_2}\left(1+\alpha^{-1}\right)\left[\,\widehat{\varepsilon}\cdot\boldsymbol{v}_{12}\,\right]\widehat{\varepsilon} \tag{2}$$

The two terms in (1) containing the prefactor $1-p$ correspond to the collisions in which, with probability $1-p$, particles do not break. The last four terms account for the fragmentation of grain 1 with mass $m_1(=\sigma_1^D)$ (resp. grain 2 with mass $m_2$), leading to the creation of two off springs with masses $um_1$ and $(1-u)m_1$ [resp. $um_2$ and $(1-u)m_2$]. Mass conservation implies a correlation between the sizes of the newborn particles.

## 3 Kinetics

A detailed analysis of the dynamics of the system, already at the Boltzmann level, according to (1), is quite involved. However, the key information is already present in the time evolution of the total density and kinetic energy densities, defined respectively as

$$n(t) = \int f(\boldsymbol{v},\sigma,t)\,d\boldsymbol{v}d\sigma \tag{3}$$

$$E_c(t) = \int v^2\sigma^D f(\boldsymbol{v},\sigma,t)\,d\boldsymbol{v}d\sigma. \tag{4}$$

The total mass density

$$M = \int \sigma^D f(\boldsymbol{v},\sigma,t)\,d\boldsymbol{v}d\sigma \tag{5}$$

is a conserved quantity and we define the temperature kinetically as

$$k_BT = \frac{2E_c}{Dn} = \frac{\langle mv^2\rangle}{D}. \tag{6}$$

In the previous equation, the angular brackets of a quantity $\mathcal{Q}$ denote the mean value $\int \mathcal{Q}f(\boldsymbol{v},\sigma,t)\,d\boldsymbol{v}d\sigma/n$.

From the Boltzmann equation, the time evolution for the density of particles reads

$$\frac{\mathrm{d}n}{\mathrm{d}t} = p\omega(t)n(t) \tag{7}$$

where $p$ is the probability that a particle breaks at a collision, and $\omega(t)$ the collision frequency

$$\omega(t) = \frac{1}{n}\int d\widehat{\varepsilon}\,d1\,d2\;\sigma_{12}^{D-1}\theta(\widehat{\boldsymbol{\sigma}}\cdot\boldsymbol{v}_{12})\,|\widehat{\varepsilon}\cdot\boldsymbol{v}_{12}|\,f(\boldsymbol{v}_1,\sigma_1,t)f(\boldsymbol{v}_2,\sigma_2,t), \tag{8}$$

where the short-hand notation $d1\,d2$ stands for $d\boldsymbol{v}_1d\sigma_1d\boldsymbol{v}_2d\sigma_2$. The kinetic energy density is unaffected by the breaking events (unlike the density itself), and only decreases due to the inelastic collisions:

$$\frac{\mathrm{d}E_c(t)}{\mathrm{d}t} \;=\; -2b_c\gamma_0\omega(t)E_c(t). \tag{9}$$

In this equation, $\gamma_0 \equiv (1-\alpha^2)/(2D)$ is related to the energy lost per collision while $b_c$ is a dimensionless collisional average

$$b_c = \frac{D}{2\omega E_c}\int d\widehat{\varepsilon}\,d1\,d2\,\theta(\boldsymbol{v}_{12}\cdot\widehat{\varepsilon})\;|\boldsymbol{v}_{12}\cdot\widehat{\varepsilon}|^3\;\frac{m_1m_2}{m_1+m_2}f(\boldsymbol{v}_1,\sigma_1,t)f(\boldsymbol{v}_2,\sigma_2,t), \tag{10}$$

where it is understood that $m_i = \sigma_i^D$. The parameter $b_c$ is a dissipation parameter: $\gamma_0 b_c$ is the ratio of the kinetic energy dissipated in an "average" collision to the instantaneous mean kinetic energy per particle. Eq. (7) expresses the fact that due to the collisions the overall number of particles in the system increases in time. In some cases, this increase is so rapid that the gas exhibits a finite-time singularity, *i.e.* the number of grains become infinite in a finite amount of time (see next section). The existence of such a singularity, which can be thought of as a limitation of the model, signaling that some of the assumptions are too simple, or that some physical ingredient is missing, will depend on the parameters that characterize the evolution of the system, $p, b_c, \alpha$ and the dimensionality $D$.

### 3.1 Scaling behaviour

We will analyze the evolution of the free evolving gas once the transient effects induced by the particular initial condition chosen have vanished. In particular, we will concentrate in the late time regime, addressing the issue whether the existence of a scaling solution is possible, where there exists a unique typical velocity and size of the particles characterizing the overall evolution of the system.

To this end, a good way to characterize the possible kinetic scenarios, is to introduce an intrinsic time scale, $\mathcal{C}$, which counts the number of collisions [7]. This scale is related to time through, $\mathrm{d}\mathcal{C} = \omega(t)\mathrm{d}t$. In terms of this variable, the evolution equations (7) and (9) read

$$\begin{aligned} \frac{\mathrm{d}n}{\mathrm{d}\mathcal{C}} &= pn(t) \\ \frac{\mathrm{d}E_c}{\mathrm{d}\mathcal{C}} &= -2b_c\gamma_0 E_c \end{aligned} \tag{11}$$

with solutions

$$n(t) = n_0 \mathrm{e}^{p\mathcal{C}} \ , \qquad E_c(t) = E_{c0}\mathrm{e}^{-2b_c\gamma_0\mathcal{C}}. \tag{12}$$

Assuming the existence of a scaling regime, the kinetics of the system is determined by one single characteristic velocity $\bar{v}(t)$, and grain size $\bar{r}(t)$. The time dependence of the distribution function $f(\boldsymbol{v}, \sigma, t)$ consequently occurs through these two quantities [up to a trivial time dependence through the density resulting from the normalization constraint (3)], and the scaling assumption amounts to restricting $f$ to the family of functions of the form:

$$f(\boldsymbol{v}, \sigma, t) = \frac{n}{\bar{r}\,(\bar{v})^D}\,\widetilde{f}(\boldsymbol{c}, \bar{\sigma}), \tag{13}$$

where we have introduced the rescaled size and velocity

$$\boldsymbol{c} = \frac{\boldsymbol{v}}{\bar{v}(t)} \quad ; \quad \bar{\sigma} = \frac{\sigma}{\bar{r}(t)}. \tag{14}$$

A natural choice is to define $\bar{v}$ as the variance of the velocity distribution and $\bar{r}$ as the mean radius: $\bar{v}^2 = \langle v^2 \rangle$, $\bar{r} = \langle \sigma \rangle$.

Within the scaling ansatz, we obtain from (10) that $b_c$ is time independent, and from (8) that $\omega$ scales with time as $n\bar{v}\bar{r}^{D-1}$ (i.e. as the ratio of typical velocity over mean free path). If we use the fact that mass density is conserved (which implies

that $\bar{r}^D n \propto M \propto t^0$), we know that $\bar{r} \propto 1/n^{1/D}$ and $\bar{v}^2 \propto E_c/M \propto E_c$. Combining these relations, we get for the collision frequency

$$\omega \propto \bar{v} n \bar{r}^{D-1} \propto \frac{\bar{v}}{\bar{r}} \propto n^{1/D} E_c^{1/2} \tag{15}$$

from which we can obtain a differential equation for the overall number of collisions as a function of time

$$\frac{\mathrm{d}\mathcal{C}}{\mathrm{d}t} = \omega_0 \left(\frac{n}{n_0}\right)^{\frac{1}{D}} \sqrt{\frac{E_c}{E_{c0}}} = \omega_0 \exp\left[\left(\frac{p}{D} - b_c\gamma_0\right)\mathcal{C}\right] \tag{16}$$

From this relation, we can obtain the explicit time dependence of the number of collisions,

$$\mathcal{C}(t) = \frac{1}{-\frac{p}{D} + b_c\gamma_0} \ln\left[1 + \left(-\frac{p}{D} + b_c\gamma_0\right)\omega_0 t\right] \tag{17}$$

Finally, the explicit time dependence of the mean number of particles and kinetic energy read

$$n(t) = n_0 \left[1 + \left(-\frac{p}{D} + b_c\gamma_0\right)\omega_0 t\right]^{p/\left(-\frac{p}{D} + b_c\gamma_0\right)} \tag{18}$$

$$E_c(t) = E_{c0} \left[1 + \left(-\frac{p}{D} + b_c\gamma_0\right)\omega_0 t\right]^{-2b_c\gamma_0/\left(-\frac{p}{D} + b_c\gamma_0\right)} \tag{19}$$

These expressions indicate when a finite-time singularity will develop. Due to mass conservation, the divergence in the number of particles implies that the mean size of the particles vanishes. We will see in the following sections that this feature may be associated with a "shattering" transition. In fact, whenever the inequality

$$-\frac{p}{D} + b_c\gamma_0 \leq 0 \tag{20}$$

holds, the number of particles diverges at a time

$$t_f = \frac{1}{\omega_0\left[\frac{p}{D} - b_c\gamma_0\right]} \tag{21}$$

at which the kinetic energy vanishes. This inequality holds at large enough fragmentation probability, $p \geq D b_c \gamma_0$. It therefore appears that the finite-time singularity cannot happen if fragmentation is just a marginal event (low $p$); alternatively, it will always be present in the elastic limit ($\alpha = 1$ so that $\gamma_0 = 0$). Hence, the kinetics of a gas of freely evolving fragmenting grains is determined by the inelasticity and the collisional average $b_c$. In principle, this collisional average is itself a function of the inelasticity; however, as discussed in the Appendix, such a dependence only appears when the velocity dependence of the distribution function $f(\boldsymbol{v}, \sigma, t)$ deviates from a Maxwellian.

In the absence of the above finite-time singularity, both $n$ and $E_c$ show power laws with time, which, from (7) in turn imposes that $\omega \propto 1/t$. The physical meaning of this remarkable feature (also observed in ballistic annihilation [2]) is that there exists a single relevant time scale in the problem. It is also noteworthy that from (15), the constraint $\omega \propto 1/t$ imposes a relation between the scaling exponents of $n$ and $E_c$.

The previous results presume the existence of a scaling regime, hypothesis that we have validated numerically, as will be described in Sect. 4. However, note that the existence of a finite-time singularity does not rule out the possibility of a scaling regime. In order to analyze quantitatively such a regime, it is useful to introduce a slower time scale, $\tau$

$$\mathrm{d}\tau = n(t)\mathrm{d}t \tag{22}$$

In this "fake" time scale, the finite-time singularity is no longer present. This feature favours the numerical analysis of the asymptotic scaling behaviour of the mixture. The internal time scale is related to $\tau$ through $\mathrm{d}\mathcal{C} = \omega \mathrm{d}\tau/n$. As a result, in terms of this new time scale, the number of collisions is expressed as

$$\mathcal{C} = \frac{1}{b_c\gamma_0 + \left(1-\frac{1}{D}\right)p} \ln\left\{1 + \left[b_c\gamma_0 + \left(1-\frac{1}{D}\right)p\right]\omega_0\tau\right\} \tag{23}$$

Hence, using the exponential growth of both the number of particles and kinetic energy in terms of the number of collisions, we get

$$n(\tau) = n_0\left\{1 + \left[b_c\gamma_0 + \left(1-\frac{1}{D}\right)p\right]\omega_0\tau\right\}^{p/\left[b_c\gamma_0+\left(1-\frac{1}{D}\right)p\right]} \tag{24}$$

$$E_c(\tau) = E_{c0}\left\{1 + \left[b_c\gamma_0 + \left(1-\frac{1}{D}\right)p\right]\omega_0\tau\right\}^{-2D/\left[D+\frac{(D-1)p}{b_c\gamma_0}\right]} \tag{25}$$

When compared with (18) and (19), one can see that, although qualitatively similar, the additional factors that characterize the exponents in this time scale ensure the absence of a finite-time singularity.

The time evolution of the physical quantities of interest in the scaling regime, as depicted in (24) and (25), depend on the inelasticity coefficient, $\alpha$, the fragmentation probability, $p$, the dimensionality, $D$, and the collisional average $b_c$. From all of these, only $b_c$ is not known *a priori*. In the Appendix, we show how it is related to the particle distribution. In particular, it is a constant for a Maxwellian distribution of velocities with a single mass-independent temperature. In this limiting case, analytic expressions for the exponents can be obtained. However, as we will see, such a factorization is too simplistic in generic situations. The collisional average will therefore have to be determined numerically, and in all cases it is the only input required to predict the corresponding exponents governing the scaling behaviour of the freely evolving gas.

Incidentally, the existence of a scaling regime can be used at one's advantage in DSMC. As has been explained previously, one of the numerical difficulties in studying the fragmentation of a freely evolving granular gas lies in the fact that the collision frequency decreases with time, making it harder to work with larger systems sizes (which is what inevitably happens in this case due to he fragmentation). On the contrary, working with the rescaled velocities $\boldsymbol{c}$ instead of the original $\boldsymbol{v}$ significantly speeds up the program, and allows to probe longer time scales [8].

### 3.2 Kinetic scenarios

As an illustration of the various kinetic scenarios covered by the previous analysis, let us consider in more detail a few limiting cases related to the kinetics of freely evolving gases.

In the absence of fragmentation, $p = 0$, obviously the number of particles remains constant, the system corresponds to that of a monodisperse granular gas, and the energy decays as

$$E_c = \frac{E_{c0}}{\left[1 + b_c \gamma_0 \omega_0 t\right]^2} \tag{26}$$

recovering Haff's law [9]. Here, the collisional parameter $b_c$ is close to 1, with deviations originating from the non-Gaussian features of the velocity distribution [15]. In this particular case, the two time scales $\tau$ and $t$ are just proportional to each other, yielding the same exponent. The assumption of spatial homogeneity prevents us from addressing the late stage deviations from Haff's law that have been described in freely evolving granular gases [9].

For an elastic gas, $\alpha = 1$, the kinetic energy is conserved. If grains can still fragment with a probability $p$, the number of particles will always diverge at a finite time,

$$n(t) = \frac{n_0}{\left[1 - \frac{p}{D}\omega_0 t\right]^D} \tag{27}$$

In this case it is easier to appreciate the advantage of introducing the slower time scale $\tau$. In terms of this variable, the number of particles will increase as

$$n(\tau) = n_0 \left[1 + \left(1 - \frac{1}{D}\right) p \omega_0 \tau\right]^{D/(D-1)} \tag{28}$$

In order to analyze the existence of an asymptotic regime (hypothesis upon which both (27) and (28) have been derived), it is more convenient to use the latter time scale, because it does not lead to a finite-time divergence. In this way, it is possible to make use of the standard techniques to address the appearance of power-law kinetic regimes, since the indefinite growth ensures the possibility to span several decades. Hence, once the algebraic regime is achieved, accurate values of the exponents can be derived as well. If such exponents are characterized, it is always possible to obtain their counterparts controlling the evolutions in the real time scale $t$.

The technique of resorting to a slower time scale will always be useful for the present class of fragmentation problems, because the exponent appearing in (24), characterizing the increase in the grain number density, is always positive for any dimension larger than 1. For $D = 1$, the elastic limit is singular. In this case, the scale $\mathcal{C}$ is proportional to $\tau$ and the number of particles increases exponentially in $\tau$ rather than algebraically. This behavior is recovered, by performing the limit $D \to 1$ in (24), and is due to the fact that in one dimension the collision frequency is proportional to the number of particles for our elastic mixture.

## 4 Numerical simulations

### 4.1 The method

We have implemented the Direct Simulation Monte Carlo technique (DSMC), which offers a particle method to solve numerically a Boltzmann-type equation, such as (1). This method was originally introduced to study rarefied gases [10], and has been extended to study granular gases [11]. It has been used in a number of different situations and it is easy to adapt to the present system, where the number of grains

increases with time. There exist already a number of applications to situations where the number of particles is not a conserved quantity, as it is the case in ballistic annihilation [2].

The assumption of spatial homogeneity simplifies further the implementation of DSMC, because it is enough to sample uniformly the relative orientation of the colliding pair, $\widehat{\varepsilon}$, without the need to keep track of the positions of the particles. Sequentially, a pair of particles is selected at random. Also the vector $\widehat{\varepsilon}$ is chosen randomly on the unit sphere and the kinematic constraint is checked. In case the particles can collide, the cross section is computed and the collision takes place proportionally to its value. The decrease in velocity of the particles due to the inelasticity reduces the cross section, hence the simulations become more expensive as time evolves. After the collision is executed (according to (2)), one of the two particles is chosen randomly, and it is broken with probability $p$.

The collision frequency of each collision $i$-$j$ can be computed on the basis of the cross-section, and hence the time is advanced accordingly at each collision

$$t \to t + \frac{1}{n^2 \, |v_{ij} \cdot \widehat{\varepsilon}| \; \sigma_{ij}^{D-1}}, \tag{29}$$

where $n$ is the instantaneous number density. It is then possible to keep track of the kinetic evolution of the system, as well as gather statistics on the distribution of sizes and velocities. In the following section we will analyze both the kinetics and the – self-similar in time– polydisperse distributions that the free evolution of the gas gives rise to.

### 4.2 Numerical results: Kinetics

We have first analyzed the kinetics in the homogeneous regime to test the scaling hypothesis discussed in Sect. 3. To this end, we have used DSMC simulations to study the evolution of a two-dimensional granular gas of circular disks with constant restitution coefficient $\alpha$. In all cases we start from an initial condition where all particles have the same size and their velocities are distributed according to a Maxwellian (monodisperse gas of elastic disks). As it has already been described in Sect. 2, we restrict ourselves to the simplest model where colliding particles fragment with a uniform probability independent of the collision properties, and where only one of the post-colliding disks fragments in two out-coming grains.

In order to validate the existence of a scaling regime, we have computed the total number of particles, $n(t)$, the collision frequency, $\omega(t)$, the mean velocity, $\langle v^2 \rangle^{1/2}$, as well as the mean radius, $\langle \sigma \rangle = \bar{r}$. We have also computed different moments of the size, $\langle \sigma^n \rangle(t)$, and velocity, $\langle v^2 \rangle^{n/2}(t)$, distribution functions. Within the scaling picture, we expect $\langle \sigma^n \rangle \propto (\bar{r})^n$ and $\langle |v|^p \rangle \propto (\bar{v})^p$, as far as the time dependence is concerned. The possibility of a multi-scaling behaviour has been reviewed by Ben-Naim and Krapivsky [12].

In Figure 1a, we display the time evolution of a few relevant quantities in the real time scale, $t$. For the parameters chosen, the system shows a finite-time singularity. As already indicated, such a phenomenon makes it difficult to assess the existence of a scaling regime, and complicates its analysis. On the contrary, when displayed in terms of the slower time scale $\tau$, as shown in Fig. 1b, one can see the existence of a scaling regime, which can be characterized. An alternative possibility to assess

the existence of a scaling regime without introducing $\tau$ would be to check if $\langle \sigma^p \rangle$ scales like $\langle \sigma^p \rangle^{n/p}$.

In Figure 2a we display different moments of the velocity distribution, as well as the mean collisional velocity $\langle v_{\rm coll} \rangle$, defined as the mean velocity modulus of colliding partners, i.e restricting to those particles that are in precollisional configurations (since a typical collision involves a particle that is "hotter" than the mean background, this quantity is larger than $\langle v \rangle$, as can be observed on the figure). Due to the inelasticity of the collisions, the typical velocity of the particles decays as a function of time. The figures show that such a decay is algebraic in $\tau$, and also that there is a single exponent characterizing different moments of the velocity. The same holds for the characteristic size of the particles as a function of time, as depicted in Fig.2b. In this case however, the scaling does not hold for negative powers of the size. We will see in the next section how such a deviation from simple scaling relates to the peculiarities of the size distribution, but it does not imply a breaking of the scaling hypothesis; it only signals the fact that moments of negative order are controlled by the smallest species in the mixture.

We can characterize the asymptotic regime by a set of exponents, that in the terms of $\tau$ can be written generically as

$$\begin{aligned} n(\tau) &\sim \tau^{\varepsilon'} \\ E(\tau) &\sim \tau^{-2\gamma'} \\ \sigma(\tau) &\sim \tau^{-\beta'}. \end{aligned} \tag{30}$$

Once these exponents are known, their counterparts associated with the $t$ scale follow. For example, using that $\mathrm{d}\tau = n_0(1+a\tau)^{\varepsilon'}\,\mathrm{d}t$, for $\varepsilon' \neq 1$ we have

$$\frac{1+a\tau}{1+a\tau_0} = \left[1 + (1-\varepsilon')\frac{n_0 a (t-t_0)}{(1+a\tau_0)^{1-\varepsilon'}}\right]^{1/(1-\varepsilon')} \tag{31}$$

from which we can derive the time evolution of any physical quantity.

In Table 1 we give the values of the exponents fitted numerically for the 2-dimensional gas at different values of the inelasticty parameter. We can determine the different exponents independently, but they are related to each other since all of them are eventually functions of the collisional average $b_c$. It is in fact rather straightforward to check that, once one of the three exponents is known, the remaining ones can be determined using the relationship between them as described in Sect. 3.

In Table 2 we list the values of the collisional average $b_c$ computed from the numerical simulations. We also display the values of the exponent $\varepsilon'$ derived using the corresponding computed values of $b_c$; comparing such values with those measured numerically (as listed in Table 1) shows a good agreement, illustrating the consistency of the analysis. The scaling hypothesis also implies, from (12), that

$$E_c \propto \left(\frac{n}{n_0}\right)^{2b_c\gamma_0/p} \tag{32}$$

which provides an alternative way to compute $b_c$ in the scaling regime (where it has to be time independent). We display in Table 2 the collisional average computed following this route [under the symbol $b_c^{(1)}$]. It shows a good agreement with

**Table 1.** Exponents characterizing the time evolution of the number and energy densities as well as the mean particle radius (see (30) for definitions) for different values of the inelasticity parameter $\alpha$, when the probability of grain fragmentation at a collision is $p = 1/2$

| $\alpha$ | $\varepsilon'$ | $\beta'$ | $\gamma'$ |
|---|---|---|---|
| 0.3 | 0.95 | 0.45 | 0.55 |
| 0.5 | 1.05 | 0.5 | 0.475 |
| 0.7 | 1.3 | 0.65 | 0.35 |
| 0.9 | 1.9 | 0.95 | 0.125 |
| 0.95 | 2.3 | 1.2 | 0.05 |

the computed collisional average, giving additional support to the existence of an asymptotic scaling regime.

In the Appendix, we have given a generic expression for $b_c$, showing that it depends sensitively on both the size and the velocity distribution of the mixture in the scaling regime. If the velocity dependence enters only through a Maxwellian, then the value of $b_c$ is independent of the mass distribution. This surprising result shows that this collisional average is a quantity that will be sensitive to deviations from Maxwell distributions. In this contribution we have only analyzed the behavior of the gas within the molecular chaos assumption, and hence, deviations of $b_c$ from unity signal a deviation from Maxwellian behavior (with the strong assumption that the temperature of a given species does not depend on its size). In a more generic study, deviations from Maxwellian behavior may also result from the breakdown of molecular chaos, so that the use of $b_c$ has to be supplemented by a second quantity that is sensitive to such a breakdown (e.g. the averaged impact parameter [13,14]).

For a mono-disperse granular gas, deviations from Maxwellian behavior vanish as the elastic limit is approached and can be described quite accurately in terms of a Sonine expansion around the Maxwellian [15]. The values of $b_c$ displayed in Table 2, on the contrary, show that the deviations from a Maxwellian velocity distribution become more pronounced as one approaches the elastic limit. This counter-intuitive trend can be traced back to the peculiar asymptotic size distribution of particles close to elasticity. Such a behavior is described in detail in the next section where it appears that the velocity distribution for nearly elastic gases deviates strongly from a global Maxwellian. At higher inelasticities, such deviations, even if always present, are not so dramatic.

### 4.3 Numerical results: Distribution functions

The existence of a scaling regime implies that the distribution function of a given quantity at two different times has to be invariant after an appropriate rescaling

**Table 2.** Collisional average $b_c$, and predicted exponent $\varepsilon'$ for different values of the inelasticity parameter $\alpha$, when the breaking probability is $p = 1/2$. $b_c^{(1)}$ is obtained from (32), plotting the kinetic energy as a function of the number of particles.

| $\alpha$ | $b_c$ | $b_c^{(1)}$ | $\varepsilon'_{\rm th}$ |
|---|---|---|---|
| 0.3 | 1.24 | 1.248 | 0.94 |
| 0.5 | 1.18 | 1.173 | 1.06 |
| 0.7 | 1.07 | 1.042 | 1.29 |
| 0.9 | 0.67 | 0.645 | 1.77 |
| 0.95 | 0.39 | 0.2318 | 1.94 |

of this quantity [see (13) and (14)]. For instance, the distribution of $\bar{\sigma} = \sigma/\langle\sigma\rangle$ is expected to be time independent. From the DSMC simulation runs, we have computed scaled distribution functions, which do indeed reach a steady state, in agreement with the scenario developed in Sect. 3. We will now discuss in detail the characteristic features of some of the relevant stationary distributions.

**Size distribution** The fragmentation process generates a polydisperse mixture of grains that evolves continuously in time, with a decreasing mean size. Large particles are consequently progressively destroyed, but the shape of the size distribution is preserved, in such a way that the relative amount of particle with respect to the time dependent mean size, $\langle\sigma\rangle(t)$, becomes independent of time.

In this regime, the scaled size distribution exhibits a marked peak for vanishingly small grains, indicating that smaller particles become predominant in the mixture. In Figure 3 we show such distributions for a number of inelasticity values, where two regions can be identified. On the extreme of large grains, the decay is exponential while it is algebraic for small particles. The exponent characterizing this algebraic behavior increases with $\alpha$. For example, for $\alpha = 0.3$ the exponent is consistent with $P(\sigma) \sim \sigma^{-0.1}$, while for $\alpha = 0.7$ we can fit the curve numerically with $P(\sigma) \sim \sigma^{-0.6}$.

It is interesting to note that at $\alpha = 0.9$, and also at $\alpha = 0.95$, the above exponent becomes close to $-1$. Such a value is peculiar, because it implies that the probability distribution is not integrable at the origin, incompatible with the requirement that $P(\sigma)$ [or $P(\bar{\sigma})$] has to be normalizable. In fact, a careful inspection of Fig. 3 shows that $P(\sigma)$ at high inelasticity develops a jump very close to the origin. Such a jump is consistent with the appearance of a singular contribution, due to a finite fraction of particles with vanishing size. This behaviour is reminiscent of a "shattering" transition [1] and is corroborated by the velocity distributions described in the next section. It indicates the development of an intrinsic size heterogeneity in the system.

The algebraic decay of $P(\sigma)$ implies that, even when the exponent is smaller (in absolute value) than $-1$, certain averages of the distribution function will not

exist. This is consistent with the behavior described in the previous section, and simply indicates that in general, averages of negative powers of the grain size will be controlled by the smallest species available in the mixture, rather than by the overall mixture. However, such a lack of scaling for certain moments of the distribution is not incompatible with the dynamic scaling behavior of the complete distribution function; rather, it shows some of the peculiarities of the asymptotic behavior of the scaling distribution (in this case at small sizes).

The existence of a stationary size distribution suggests the possibility to map the fragmenting granular gas onto an effective polydisperse mixture with a time dependent mean. Although this is indeed possible in principle, we do not have any theoretical framework (except the complicated initial Boltzmann equation) to predict either the algebraic decay of $P(\sigma)$ or the details of the exponential tail.

**Velocity distribution** We have also studied the velocity distribution to assess how relevant deviations from Maxwellian are, and also to analyze the meaning of a global temperature characterizing the whole system.

In Figure 4 we display the distribution of rescaled velocities $\boldsymbol{c}$ at different inelasticities. Deviations from Maxwellian behavior are observed at all values of $\alpha$. However, the deviations become more prominent close to the elastic limit, in agreement with the development of a singular contribution coming from vanishingly small grains, explaining the small values for $b_c$ listed in Table 2. In order to gain more insight, we have also computed separately the velocity distribution from those particles with a mass smaller than 5% the mean mass. In Figure 5a we compare the overall velocity distribution with that of the smaller particles and the contribution coming from the rest of the grains for $\alpha = 0.95$. The two subsets behave more closely to a Maxwellian than the mean velocity distribution. The low velocity part of the distribution is controlled by the contribution from most of the particles, while the large velocity part is dominated by the small particles. These are characterized by a much larger temperature than the mean, while the rest of the species are much colder (large particle have suffered a low number of collisions (and hence of fragmentations), which requires that they were among the very "cold" ones initially).

Although less dramatic, the same trend is observed for all values of $\alpha$. For example, in Fig.5b we display the equivalent distribution functions at $\alpha = 0.5$. In this case, again the two subsets of grains evolve following separate approximate Maxwellians. According to this interpretation, as $\alpha$ increases, the separation in temperates between the two sets of particles increases.

Such an inhomogeneous dependence of the velocity distribution (and in particular its second moment) on grain species, explains the large deviations of $b_c$ from the Maxwellian prediction reported close to the elastic limit. These results also cast doubts on the use of a single temperature to characterize a polydisperse granular mixture. Nonetheless, it is worth noting that such a size heterogeneity does not affect the scaling hypothesis. Even if different temperatures could be defined for different subsets of particles, all of them have the same time evolution, explaining why it is possible to have a simple velocity scaling. Such a behavior has been reported for the free evolution of bidisperse granular mixtures [16]. However, the absence of a common temperature invalidates the use of perturbative calculations, e.g. through a Sonine expansion, to determine the deviations from Gaussian behav-

ior as the inelasticity is increased, as is customary in the case of monodisperse (and even bidisperse) granular gases.

## 5 Discussion

We have investigated the evolution of a granular gas in the absence of any driving, taking into account the possibility that the collisions may lead to a fragmentation of the impacting grains.

Rather than performing a detailed analysis of the fragmentation process, we have analyzed the simplest possible model, where the fragmentation is a random event uncorrelated to the details of the collision, except for the requirement that only colliding particles may fragment. This simple fact already leads to a number of interesting results. We have shown the existence of a scaling homogeneous regime characterizing the kinetics of the system. Such a regime is controlled eventually by a single collision average, $b_c$. The relevance of $b_c$ in the asymptotic regime shows that a theory based on rate equations, usually disregarding collision induced correlations, will be too simplistic to capture the dynamics in these systems.

We have shown how the evolution in the scaling regime may lead to a finite-time singularity where the number of particles diverges. We have derived the conditions leading to this finite-time catastrophe, depending on the different parameters that characterize the system. In the absence of such a singularity, the various moments of the size and velocity distribution exhibit algebraic scaling laws with time, that can be regarded as a generalized Haff's law.

The size distribution exhibits two different limiting kinds of behaviour: an exponential tail at large sizes (compared to the time dependent mean size), and a power-law distribution for small sizes, which may develop into delta singularity close to the elastic limit. The details and character of such a transition, which has been reported in other fragmenting systems [1] deserve a more careful analysis. The existence of a scaling regime is not incompatible with the presence of marked size heterogeneities in the mixture. In particular, the characteristic temperature of small and large grains can be significantly different, in such a way that the mean scaled velocity distribution cannot be regarded as a slightly distorted Maxwellian.

In order to assess to which extent the results discussed are specific of the fragmentation mechanism that has been chosen, we have also carried out numerical studies for a model where the fragmentation probability is correlated to the energy lost in a collision [17]. In that case there exists still a scaling regime characterizing the kinetics. The scaled distribution functions are also similar, except for the fact that size distributions are closer to an exponential. Hence, the results obtained through the analysis of the simplest model provide a reference system, against which other models can be tested, and in this way it should be possible to disentangle the generic aspects involved in the dynamics of fragmenting granular materials.

Acknowledgments: We would like to thank A. Barrat for useful discussions. I.P. acknowledges the support of CNRS through the attribution of a "poste de chercheur associé", and the hospitality of the "Laboratoire de Physique Théorique" in Orsay where most of this work was performed.

## Appendix: On the collisional average $b_c$

The kinetics of the free fragmenting granular gas depends on the value of the collisional average $b_c$, which in turn is a complicated function of the joint size and velocity distribution. To proceed further, we assume that in the scaling regime, the velocity dependence is Maxwellian. From the distribution function $f(\boldsymbol{v},\sigma,t)$, we change variables and introduce the joint distribution of masses and velocity $f(m,\boldsymbol{v},t)$ that we approximate by

$$f(m_i,\boldsymbol{v}_i,t) \simeq \psi(m_i,t)\phi(m_i v_i^2,t) \tag{33}$$

where $\psi$ is the mass distribution, while $\phi(m_i v_i^2)$ is the Maxwellian,

$$\phi(m_i v_i^2,t) = \left(\frac{\beta m_i}{2\pi}\right)^{D/2} \mathrm{e}^{-m_i v_i^2 \beta/2}. \tag{34}$$

The time dependence of $\phi$ is encoded in $\beta = 1/(k_B T)$, see (6). The key assumption here is that $k_B T$ does not depend on the mass $m$, as would be the case in an equilibrium polydisperse system. We have

$$b_c = \beta \frac{\int \mathrm{d}1\,\mathrm{d}2\,\mathrm{d}\widehat{\varepsilon}\,\theta(\boldsymbol{v}_{12}\cdot\widehat{\varepsilon})\,|\boldsymbol{v}_{12}\cdot\widehat{\varepsilon}|^3\,\sigma_{12}^{D-1}\mu_{12}\psi(m_1)\phi(m_1v_1^2)\psi(m_2)\phi(m_2v_2^2)}{\int \mathrm{d}1\,\mathrm{d}2\,\mathrm{d}\widehat{\varepsilon}\,\theta(\boldsymbol{v}_{12}\cdot\widehat{\varepsilon})\sigma_{12}^{D-1}\psi(m_1)\phi(m_1v_1^2)\psi(m_2)\phi(m_2v_2^2)} \tag{35}$$

where d1 stands for $\mathrm{d}\boldsymbol{v}_1\,\mathrm{d}m_1$. We can express the collisional average $b_c$ in dimensionless quantities, and also transform the velocities to express them in terms of the center-of-mass and relative coordinates. One arrives at

$$\begin{aligned} b_c &= \frac{2\beta}{(D+1)} \frac{\int \mathrm{d}\boldsymbol{c}\mathrm{d}m_1\mathrm{d}m_2 c^3 \sigma_{12}^{D-1}\mu_{12}\psi(m_1)\psi(m_2)(m_1m_2)^{D/2}\mathrm{e}^{-\beta\mu_{12}c^2/2}}{\int \mathrm{d}\boldsymbol{c}\mathrm{d}m_1\mathrm{d}m_2 c\sigma_{12}^{D-1}\psi(m_1)\psi(m_2)(m_1m_2)^{D/2}\mathrm{e}^{-\beta\mu_{12}c^2/2}} \\ &= \frac{\int \mathrm{d}m_1\mathrm{d}m_2 \left(\frac{1}{\mu_{12}}\right)^{\frac{D+3}{2}} \mu_{12}\,\sigma_{12}^{D-1}\,\psi(m_1)\psi(m_2)(m_1m_2)^{D/2}}{\int \mathrm{d}m_1\mathrm{d}m_2 \left(\frac{1}{\mu_{12}}\right)^{\frac{D+1}{2}} \sigma_{12}^{D-1}\,\psi(m_1)\psi(m_2)(m_1m_2)^{D/2}} = 1 \end{aligned} \tag{36}$$

where use has been made of

$$\int \mathrm{d}\widehat{\varepsilon}\theta(\boldsymbol{c}\cdot\widehat{\varepsilon})\,|\boldsymbol{c}\cdot\widehat{\varepsilon}|^n = \frac{\pi^{\frac{D-1}{2}}\Gamma\left(\frac{n+1}{2}\right)}{\Gamma\left(\frac{n+D}{2}\right)}\,c^n \tag{37}$$

So, $b_c = 1$ if the velocity distribution follows a Maxwellian. Hence, this collisional average is a good measure of deviations from Maxwellian behavior in polydisperse granular gases.

## References


1. S. Redner *Fragmentation* In H.J Hermann and S. Roux, editors, *Statistical Models for the Fracture of Disordered Media*, 1990, Elsevier Science Pubs. (North Holland).
2. E. Trizac *Phys. Rev. Lett.* **88**, 160601 (2002).
3. J. Piasecki, E. Trizac and M. Droz, *Phys. Rev. E* **66** 066111 (2002)

4. P. Résibois and M. de Leener, *Classical Kinetic Theory of Fluids*, John Wiley and Sons (1977).
5. I. Goldhirsch and G. Zanneti *Phys. Rev. Lett.* **70**, 1619 (1993).
6. V. Buchholtz, J.A. Freund and T. Pöschel. *Europ. Phys. J. B* **16**, 169 (2000).
7. S. McNamara and W.R. Young, *Physics of Fluids* **5**, 34 (1993).
8. J.M. Montanero and A. Santos, *Granular Matter* **2**, 53 (2000).
9. R. Brito and M.H. Ernst *Europhys. Lett.* **43**, 497 (1998).
10. G. Bird *Molecular Gas Dynamics and the Direct Simulation of Gas Flows* Clarendon Press, Oxford, 1994.
11. J.M. Montanero, V. Garzó, A. Santos and J.J. Brey, *J. Fluid Mech.* **389**, 391 (1999).
12. E. Ben-Naim and P.L. Krapivsky, Physica D **107**, 156 (1997).
13. S. Luding, ZAMM **80**, 9 (2000).
14. I. Pagonabarraga, E. Trizac, T.P.C. van Noije and M.H. Ernst *Phys. Rev. E*,**65**, 011303 (2002).
15. T.P.C. van Noije and M.H. Ernst *Granular Matter* **1**, 57 (1998).
16. V. Garzó and J. Dufty *Phys. Rev. E* **60**, 5706 (1999).
17. I. Pagonabarraga and E. Trizac *in preparation*

## Figure Captions

**Fig. 1.** Time evolution in linear-log scale of the total number of particles, mean size and characteristic velocities for $\alpha = 0.5$, and a fragmentation probability $p = 1/2$ in $D = 2$. **(a)** Time evolution as a function of the real time scale $t$; **(b)** Time evolution in a log-log scale in terms of the slow time scale $\tau$. The thin lines correspond to the fitted power-laws for the different quantities.

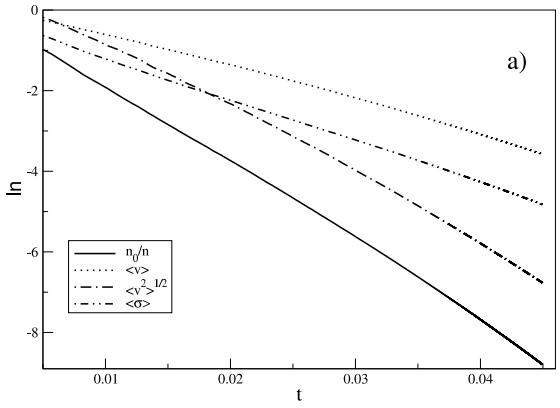
**Fig. 2.** Time evolution of different moments of the **(a)** velocity distribution function, and **(b)** size distribution function for the same parameters as Fig. 1. In **(a)** the time evolution of the mean velocity of colliding grains is also depicted. In both cases the slow time scale is used, and the corresponding fitted power-law decays are displayed as thin lines.

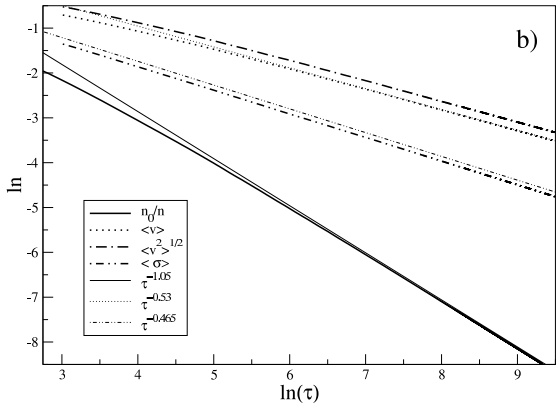
**Fig. 3.** Log-log plot of the rescaled particle radius distribution, for a uniform random fragmentation probability $p = 1/2$ in $D = 2$.

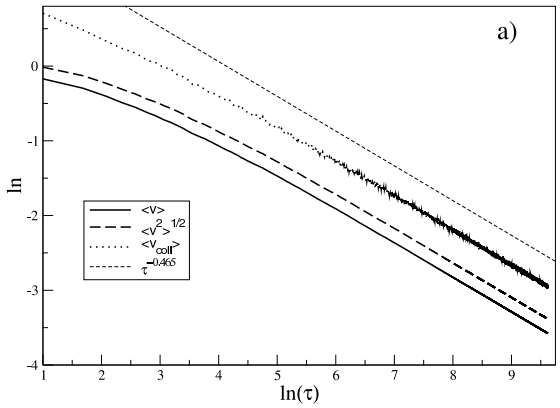
**Fig. 4.** Linear-log plot of the rescaled velocity distribution $\mathbf{c} = \mathbf{v}/\bar{v}$.

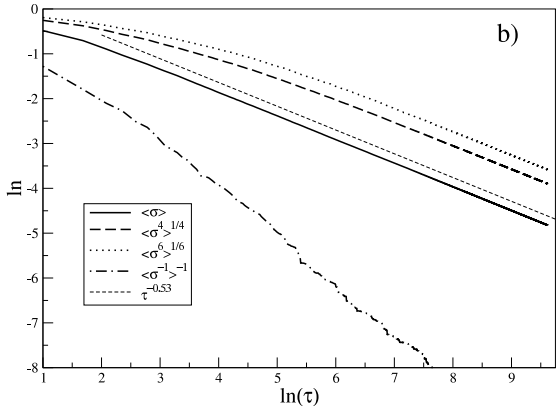
**Fig. 5.** Linear-log plot of particle velocity distributions, scaled by the mean velocity, for a uniform fragmentation probability. "Small" refers to the distribution of velocities for particles having a mass smaller than 5% the mean mass. "Large" corresponds to the distribution of the rest of the grains. **(a)** $\alpha = 0.95$; **(b)** $\alpha = 0.5$

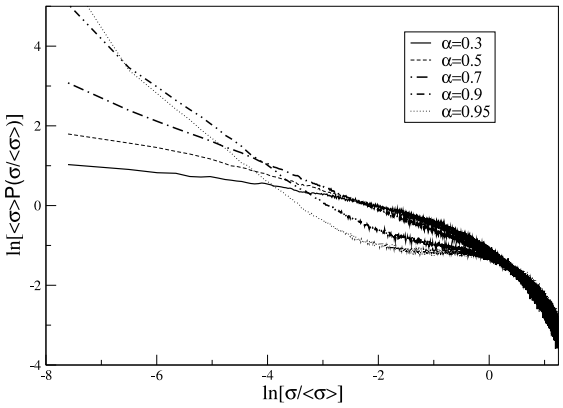
## Figures

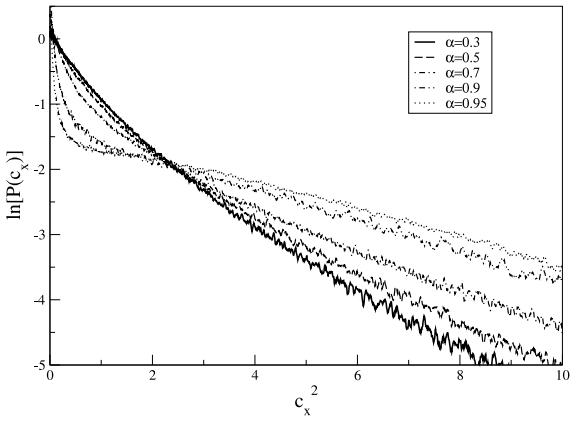


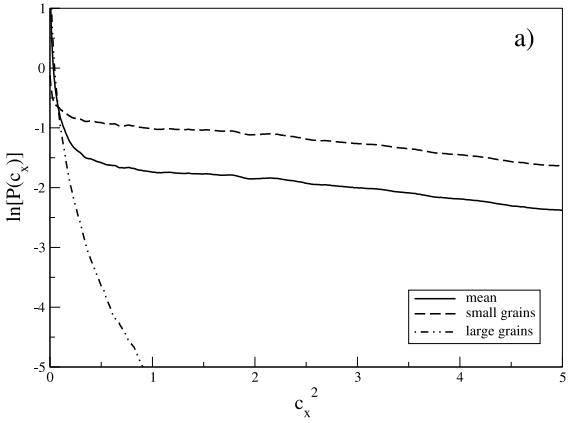



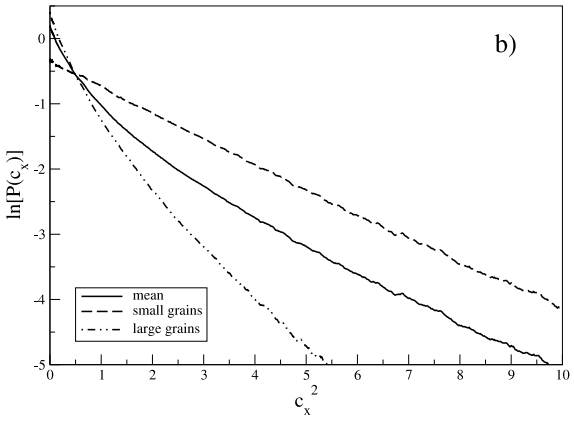

a)
ln
ln(τ)
<v>
<v^2>^1/2
<v_coll>
τ^-0.465


b)
ln
ln(τ)
<σ>
<σ^4>^1/4
<σ^6>^1/6
<σ^-1>^-1
τ^-0.53


α=0.3
α=0.5
α=0.7
α=0.9
α=0.95
ln[<σ>P(σ/<σ>)]
ln[σ/<σ>]
4
2
0
-2
-4
-8
-6
-4
-2
0


α=0.3
α=0.5
α=0.7
α=0.9
α=0.95
ln[P(c_x)]
c_x^2
0
-1
-2
-3
-4
-5
0
2
4
6
8
10


a)
ln[P(c_x)]
c_x^2
mean
small grains
large grains


b)
ln[P(c_x)]
c_x^2
mean
small grains
large grains